Prism Signal Processing for Machine Condition Monitoring II:

Experimental Data and Fault Detection

Manus Henry, Vladimir Sinitsin

Accepted for 1st IEEE International Conference on Industrial Cyber-Physical Systems (ICPS 2018), Saint Petersburg, Russia, May 15-18, 2018.

Prism Signal Processing for Machine Condition Monitoring II: Experimental Data and Fault Detection

Manus Henry[a,b]
[a]University of Oxford
Oxford, OX1 3PJ, UK.
manus.henry@eng.ox.ac.uk

Vladimir V Sinitsin[b]
[b]South Ural State University (SUSU)
Chelyabinsk, Russia.
a160403@gmail.com

***Abstract*— The Internet of Things (IoT) concept, alongside wireless technologies, supports the mounting of sensors in inaccessible positions and thus provides new opportunities for machine condition monitoring. This paper outlines experimental results using Prism signal processing to track rotor angular acceleration via a Wireless Acceleration Sensor (WAS) mounted on a rotating shaft. The instantaneous frequency and amplitude of each component of the angular acceleration is tracked, with a view to providing diagnostic information. The experimental results illustrate how amplitude data can provide indications of gear faults, via further Prism signal processing.**

Keywords*— *Prism signal processing, diagnostics, accelerometer, wireless acceleration sensor, rotating machinery.

I. INTRODUCTION

Gears are widely used mechanical components with a significant impact on machine reliability and efficiency. Gear fault detection and diagnosis is thus an important theme in machine condition monitoring. Vibration monitoring via acceleration measurement is the most widely used approach for gear condition monitoring. However, the influence of machine workloads on gear vibration levels may complicate the application of traditional methods, such as RMS and Kurtosis, which compare via various signal parameters the 'healthy machine state' with the 'current machine state' [1]. Therefore, researchers use special methods, such as Time Synchronous Averaging (TSA) [2], wavelet analysis [3], the Hilbert transform [4], Empirical Mode Decomposition (EMD) [5] and combinations of those methods [6-8]. Unfortunately, these methods are limited by sensitivity to the machine's operating speed and/or a requirement for high computational resources.

Alongside traditional vibration monitoring (accelerometers mounted on the housing near the bearings), researchers have proposed tracking the instantaneous angle of rotation using precision optical encoders [9, 10]. Typically the encoders are fixed to the gear shaft, which limits the application of the approach. However, wireless technologies and the IoT concept offer the possibility of combining traditional measurements with angle tracking within a single sensor system, for example the Wireless Acceleration Sensor (WAS) [11]. In earlier work, WAS systems have been mounted on moving elements (for example the gear). Sensor data and power are transferred wirelessly. WAS contains several MEMS-accelerometers with different orientations, so that the linear angular acceleration of the gear can be measured simultaneously. The WAS prototype showed high sensitivity to rolling bearing faults [12]. However, the implementation of wireless technologies into the sensor limits computational resources and, accordingly, requires low computing cost methods to track signal changes in real time.

The Prism [13] offers low cost and highly flexible signal processing. In our companion paper [14] Prism was applied to the tracking of a rotor angular acceleration via a WAS, where the angular acceleration signal has eight frequency components. The instantaneous frequency and amplitude of each component was tracked, providing diagnostic information.

The rotor system used for experimental work operates in a series of 'runs', consisting of a *startup* period where the rotor begins movement and accelerates to the desired rotation speed (usually via an overshoot), followed by a period of more or less *steady* operation at approximately the desired rotational speed.

The Prism-based signal processing scheme is designed to match the requirements of this application. For the startup period, only the (variable) operating frequency is needed, in order to establish the transition to the steady mode and to determine the steady rotation speed. A Prism-based Recursive

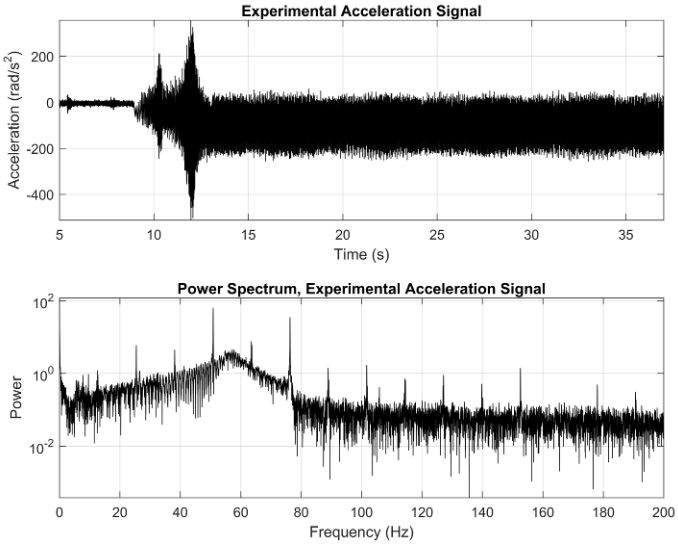

Fig. 1. Typical acceleration data for rotor run at 12 Hz.

The work was supported by Act 211 Government of the Russian Federation, contract № 02.A03.21.0011

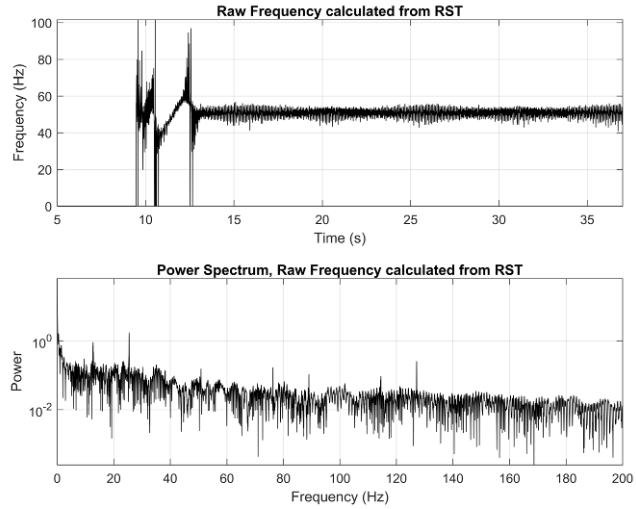

Fig. 2. Raw frequency measurement from experimental data at 12 Hz

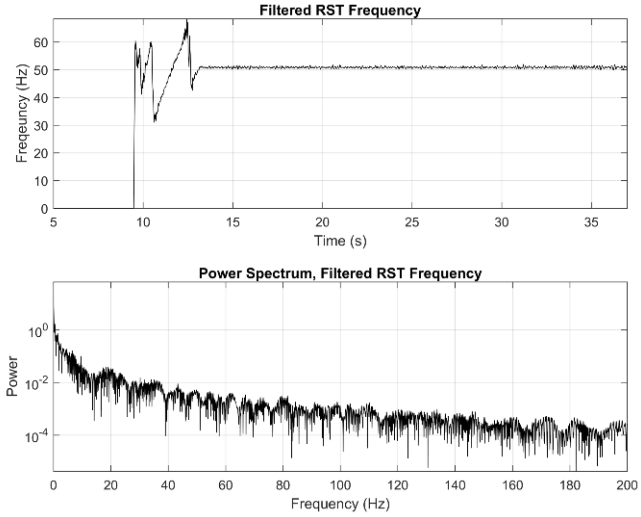

Fig. 3. Filtered frequency measurement from experimental data at 12 Hz

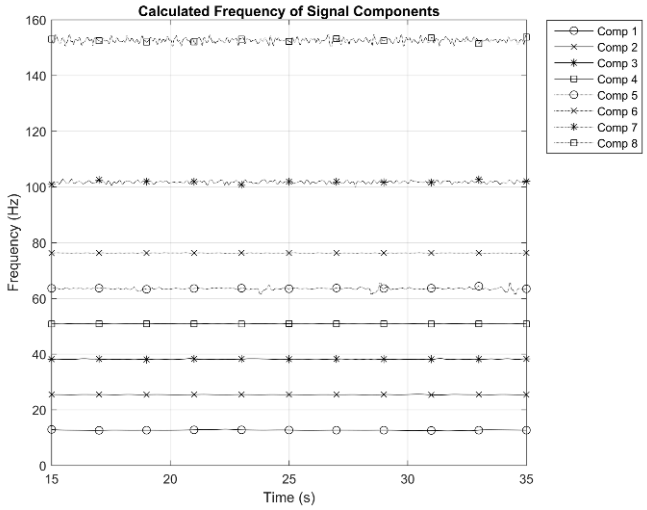

Fig. 4. Component frequencies from experimental data at 12 Hz

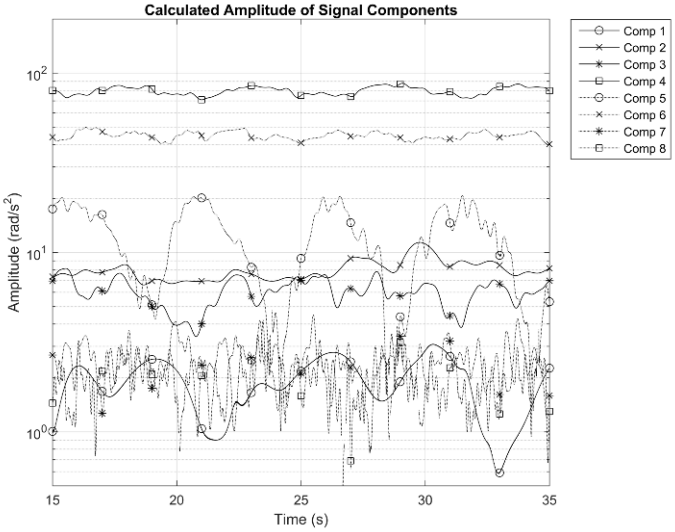

Fig. 5. Component amplitudes from experimental data at 12 Hz

Signal Tracker (RST) is able to track the frequency during the startup period, but the measurement is heavily contaminated due to the presence of multiple frequency components in the acceleration signal. The simple provision of an FIR moving average filter with window length set to the observed period of rotation significantly reduces the frequency noise, facilitating good tracking with simulated data. For steady operation, Prism-based bandpass filtering is used to isolate each frequency component prior to separate RST calculation of frequency and amplitude. The key feature here is that the low cost of Prism filter design facilitates the creation of new filters around the current operating frequency for each run.

II. Variable Speed Experimental Data

In this paper, experimental data is used to confirm the utility of the Prism-based scheme for gear fault diagnosis. Firstly, its operation is demonstrated with fault-free data at two different operating speeds. Secondly, the detection of gear faults is investigated, where it is shown that further Prism processing of the amplitude data, may form the basis of an effective fault detection scheme. Figure 1 (from [14]) shows typical data for a rotor experiment with a final steady rotation speed of about 12 Hz. The power spectrum shows the most significant signal components, all at multiples of the rotation frequency, with the highest amplitude at the fourth harmonic.

Figs. 2 and 3 show the rotor frequency tracked by the first RST, before and after the application of the moving average filter. The filtered frequency is much cleaner, showing, after an initial transient, linear trends during the startup period and a reasonably constant value for the subsequent period of steady operation. The corresponding power spectra demonstrate that the harmonics have been removed by the moving average filter.

Figs. 4 and 5 show the results of the second stage signal processing, whereby, for each component to be tracked, a bandpass filter and RST is designed in real time, based on the observed (initial) steady frequency of Fig. 3. The frequency and amplitude values are updated once per sample, i.e. at 41 kHz. Fig. 4 shows that the frequency of each component remains reasonably constant during steady operation, while Fig. 5 shows that the amplitude behaviour of the components is more complex. Some exhibit fairly stationary amplitude, while others show random and/or pseudo-periodic behavior. For example, the highest amplitude components, corresponding to the 4^{th} and 6^{th} harmonics respectively, show a low level of

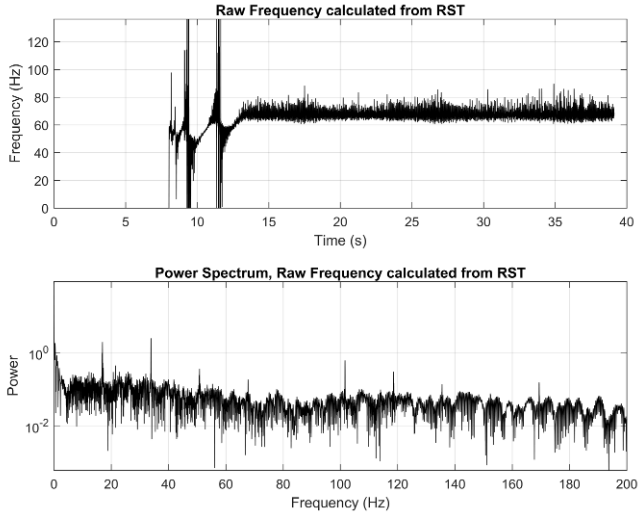

Fig. 6. Raw frequency measurement from experimental data at 16 Hz

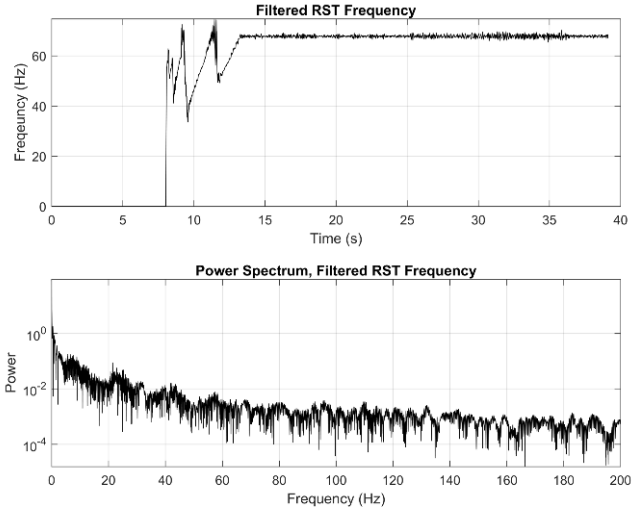

Fig. 7. Filtered frequency measurement from experimental data at 16 Hz

oscillation around a mean value; the 5th component shows a higher degree of oscillation; the 6th component is relatively flat, and the other components have more random variation.

The time-varying behavior of the amplitude parameters suggest a rich set of characteristics that might be used for fault detection, as discussed in the next section. However, a more basic requirement is to demonstrate that this signal processing scheme is able to manage different rotor speeds. Accordingly, Figures 6 and 7 show the raw and filtered frequency for another experiment in which the final steady frequency is around 16 Hz. The same signal processing scheme successfully tracks the variable frequency during the startup period, which exhibits several linear shifts before settling to a steady frequency, which, for the 4th harmonic, is around 64 Hz.

III. Diagnostic Data for Gear Faults

The gear system is a common fault source in rotating machinery. Trials have been carried out on the experimental rotor system where the normal, fault-free bevel gear has been replaced by a unit with either a worn or a broken gear tooth (Fig. 8). To detect these faults, the accelerometer disk is mounted on the gear housing (Fig. 9). The resulting signals, in the absence of faults, have a broadly similar characteristic to those of Fig. 1, but with certain differences.

Fig. 8. Broken tooth on bevel gear

Fig. 10 shows the acceleration signal and its power spectrum for a typical run with a healthy gear. The signal has a significantly higher level of noise, with the noise floor rising with frequency. There are additional, aharmonic peaks present in the spectrum. Furthermore it is the 6th rather than the 4th harmonic that has the highest amplitude. While it would be straightforward to track the 6th harmonic instead of the 4th, the noise at high frequency poses a bigger challenge, which is met by the simple expedient of using a low pass (Prism-based) filter in the startup tracking phase in order to reduce the influence of both the 6th harmonic and the high frequency noise. Space constraints prevent the inclusion of additional plots, but the results are broadly similar to Figures 6 and 7.

Given the potential to track the frequency and amplitude of the eight signal components in real time, it is possible to look for useful diagnostic indicators. Here we considered three conditions: a normal, fault-free gear; a gear with a chipped tooth; and a gear with a broken tooth (Fig. 8).

Figs. 11 – 15 show the time series obtained for the amplitudes of the 1st, 2nd, 4th, 5th, and 6th frequency components respectively for each of the different diagnostic conditions. These demonstrate a variety of behaviours, which in some cases vary with the diagnostic condition. Several (but not all) of the amplitude time series show strong oscillatory behaviour,

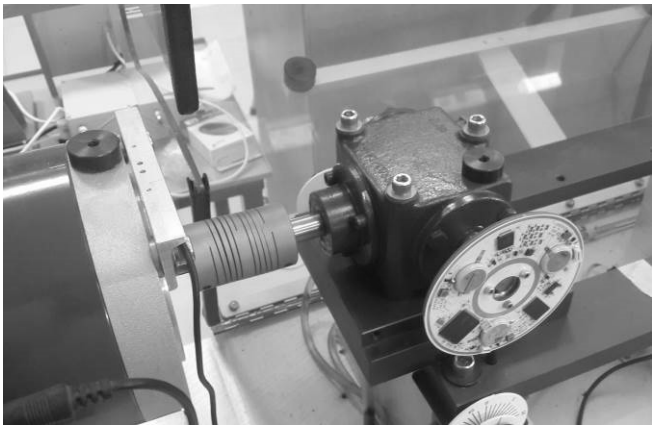

Fig. 9. PCB sensing board mounted on gear housing to detect gear faults

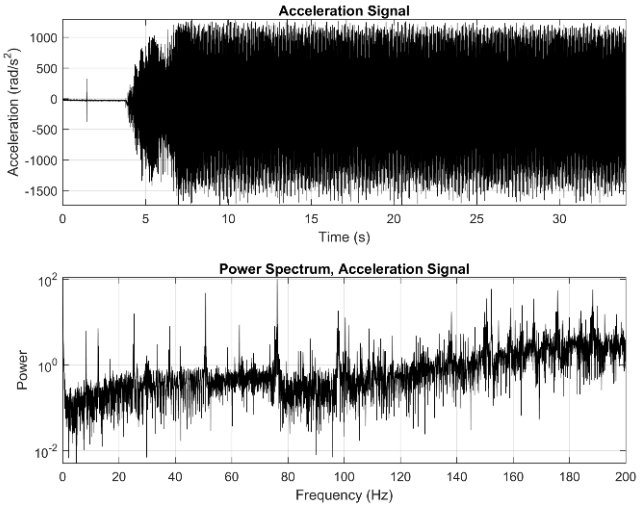

Fig. 10. Typical acceleration data for rotor run at 12 Hz, with sensor mounted on gear housing and with no gear fault.

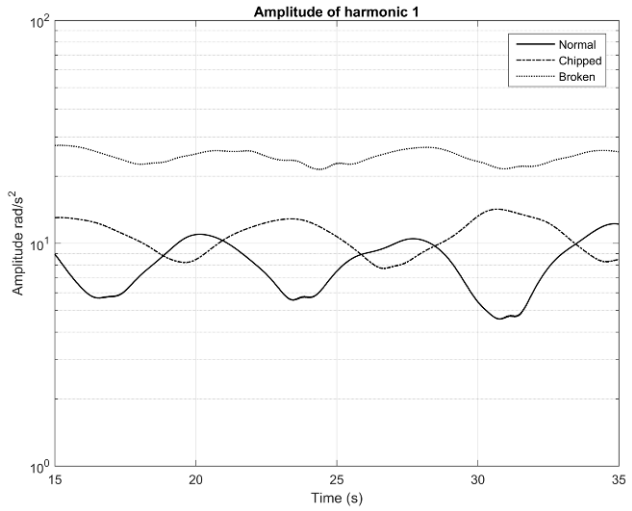

Fig. 11. Time series of 1st harmonic amplitude for different gear faults; steady rotor speed 12 Hz.

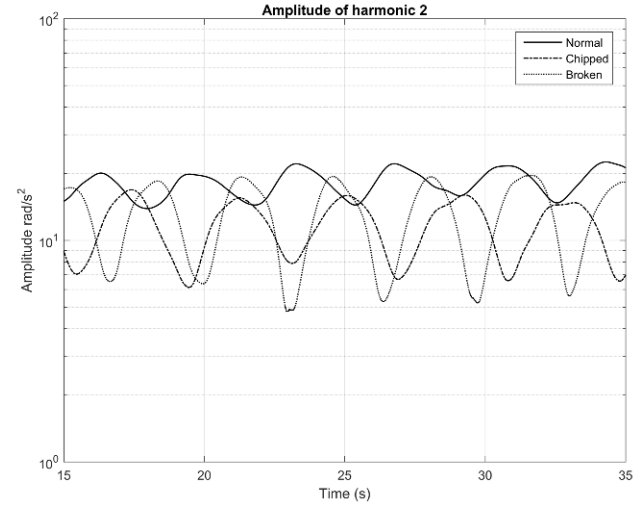

Fig. 12. Time series of 2nd harmonic amplitude for different gear faults; steady rotor speed 12 Hz.

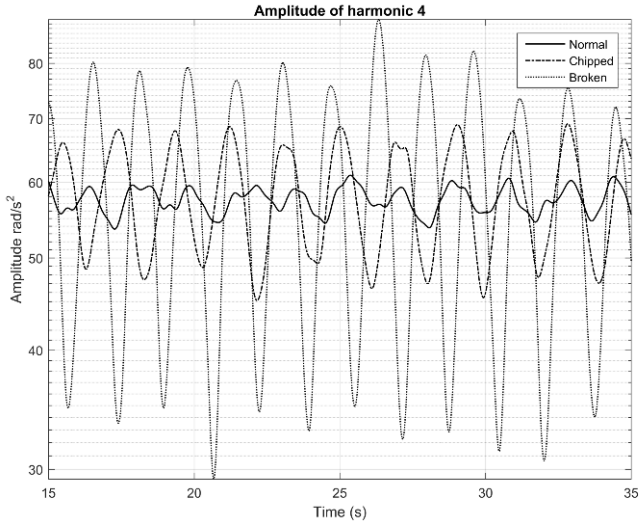

Fig. 13. Time series of 4th harmonic amplitude for different gear faults; steady rotor speed 12 Hz.

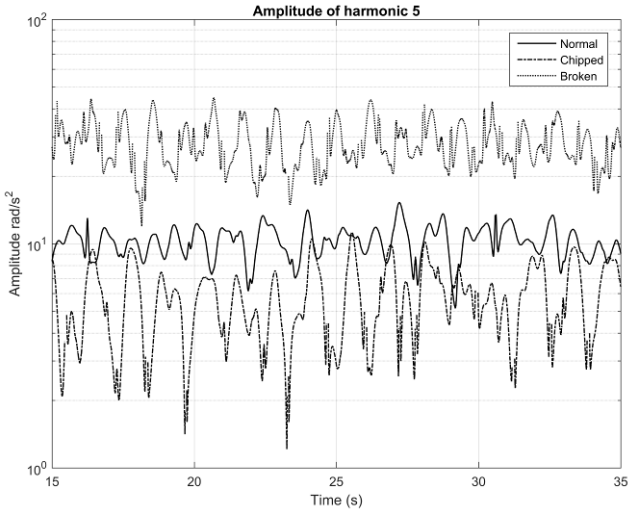

Fig. 14. Time series of 5th harmonic amplitude for different gear faults; steady rotor speed 12 Hz.

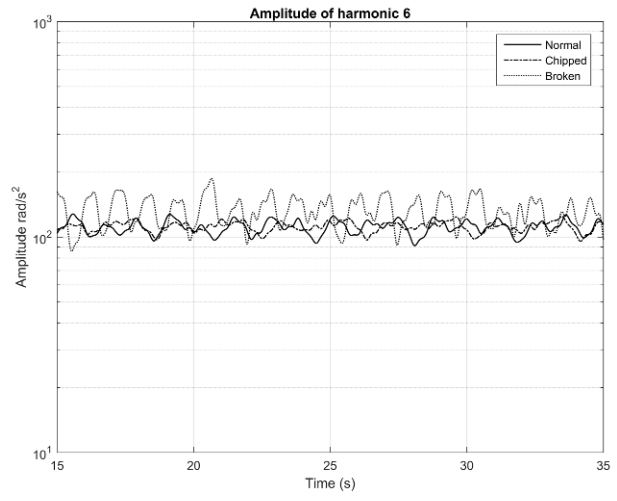

Fig. 15. Time series of 6th harmonic amplitude for different gear faults; steady rotor speed 12 Hz.

whereby the mean value (i.e. DC offset), the frequency and/or the amplitude of oscillation are different in each case for the healthy gear, the worn tooth and the chipped tooth.

For example, for the 1st and 5th harmonics (Figs. 11 & 14), the mean value of the amplitude shifts with the diagnostic condition. For the 1st harmonic, the average amplitude is higher for the chipped gear tooth than for an intact gear, and higher again for the broken tooth. In Fig. 14, any sinusoidal variation is obscured by random variation; the average amplitude is lower for the chipped gear tooth case than for the healthy gear, but the broken gear tooth case still generates the highest average 5th component amplitude.

Figs. 12 and 15 show the 2nd and 6th harmonics respectively. These display relatively little variation in properties with tooth damage. It is perhaps surprising that the 6th harmonic, which is the dominant component in the signal, shows little change with either a chipped or a broken tooth.

Fig. 13, showing the 4th harmonic, exhibits the most interesting behaviour. Here, while the mean amplitude appears to be relatively constant for the different diagnostic conditions, the amplitude of the signal modulation increases significantly from the normal to the chipped to the broken cases.

A variety of techniques could be applied to develop a systematic diagnostic analysis of the rotor machine, based upon the amplitude information provided by the Prism signal processing scheme. Such work would require a large experimental program and an analysis that is beyond the scope of the current paper. However, the next section will demonstrate how a further stage of Prism signal processing may be used to characterize the oscillatory behavior of the 4th harmonic shown in Figure 13.

IV. Higher Level Prism Signal Processing

As the parameter values (frequency, amplitude and/or phase) generated from a Prism-based tracker are updated once per sample, these outputs can be treated as additional time series which may in turn be subject to further analysis. For example, in [15], a Prism-based fault detection scheme is described for a resonant sensor. In this case, the frequency output of a RST tracker is fed into a second RST to detect any resonances indicative of any additional, undesired frequency component in the original signal. Should this fault be detected, then additional Prism signal processing stages are instantiated to track and remove the undesired signal component.

As shown in Fig. 16, a multi-stage signal processing scheme can be used to extract the sinusoidal parameters of the time varying amplitude of the 4th harmonic (from Fig. 13). This assumes that the steady phase of the rotor's operation has commenced and that the rotation frequency is known to a reasonable approximation. The acceleration signal s(t) is first passed through a bandpass filter, centred on the expected frequency of the 4th harmonic. The resulting filtered signal $s_{filt}(t)$ is then passed into a first RST to generate sample-by-sample estimates of the 4th harmonic frequency (labelled $f^4(t)$) and amplitude (labelled $A^4(t)$). This amplitude signal $A^4(t)$ is as shown in Fig. 13, for the different diagnostic conditions tested experimentally.

The subsequent signal processing stages in Fig. 16 are used to extract the frequency (labelled $f_{A4}(t)$) and amplitude of oscillation (labelled $A_{A4}(t)$) of $A^4(t)$. This is achieved using a low pass Prism-based filtering stage where the characteristic frequency has been set at 2 Hz, thus removing high frequency jitter, followed by a further RST tracker stage.

Figs. 17 and 18 show the resulting time series of $A_{A4}(t)$ and $f_{A4}(t)$ for the same experimental data as shown in Fig. 13. The modulation frequency (Fig. 17) varies between 0.45 Hz and 0.65 Hz. For the normal, fault free case, the modulation frequency moves between these two limits. By contrast, the frequencies observed for the chipped and broken gear tooth case are more steady, with values of approximately 0.525 Hz and 0.625 Hz respectively.

Fig. 18 shows the amplitudes of the modulation for the fourth harmonic for the different cases of gear tooth fault. None of the data suggests further oscillation, although there is some degree of random drift. Nevertheless, the distinction between the three cases is very clear: the fault free case has an average amplitude of approximately 2.5 rad/s^2; the chipped gear tooth case has an average amplitude of approximately 10 rad/s^2; and the broken gear tooth case has an average amplitude of approximately 22.5 rad/s^2. The variation in each signal is low compared to the differences between the results from each experiment, suggesting that this parameter could be a useful indicator of the diagnostic state of the gear system.

As stated above, the current aim of the project is to demonstrate the viability and utility of Prism signal processing techniques for detecting faults in rotating machinery. Future work will include identifying a comprehensive set of diagnostic parameters for a wider set of fault conditions, and developing the corresponding diagnostic reasoning. A further goal is a real-time implementation of Prism signal processing on the accelerometer card (Fig 9).

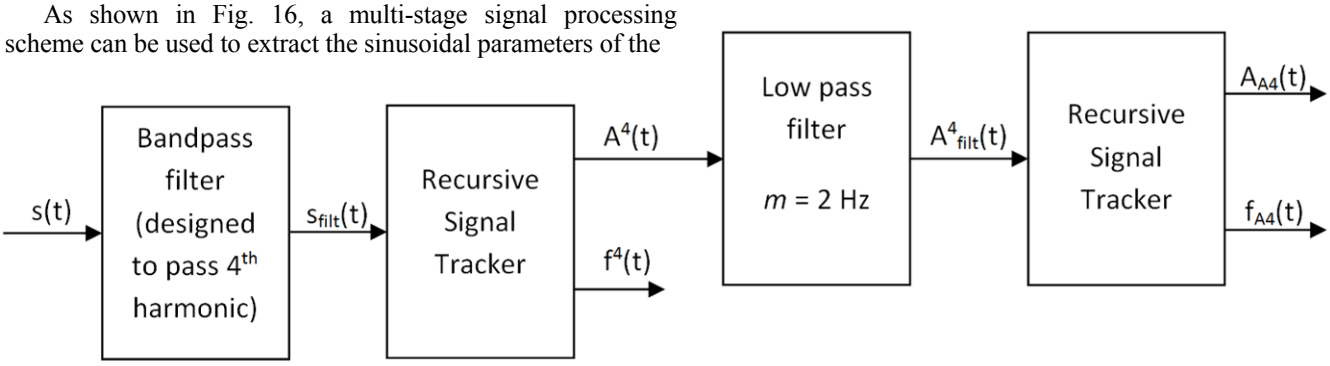

Fig. 16. Signal Processing Scheme to track fourth harmonic

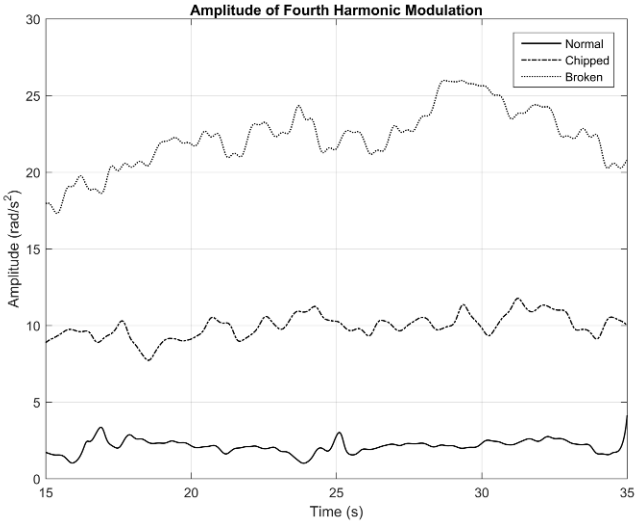

Fig. 17. Modulation frequency of 4th Harmonic data with gear faults, and with 12 Hz steady operating frequency

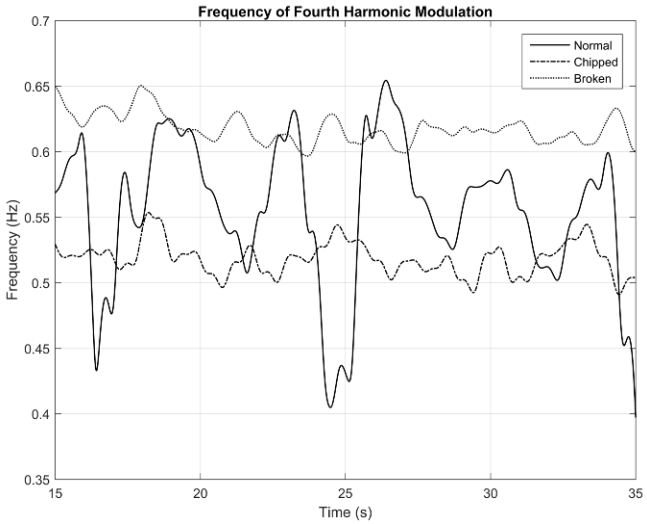

Fig. 18. Modulation amplitude of 4th Harmonic data with gear faults, and with 12 Hz steady operating frequency

V. Discussion

The IoT requires fast and flexible signal processing techniques. A key to flexibility is rapid and low-cost filter design that can be carried out in real time in order to adapt to current signal properties. This paper has provided a simple worked example of how Prism signal processing can provide the required flexibility and low-cost real-time design.

The two-stage signal processing design - startup tracking followed by the monitoring of all signal components during the steady phase – is only possible because the second stage components (bandpass filters and RST trackers) can be designed and instantiated in real time to match the steady operating frequency at the start of the second stage.

The accelerometer card is a wireless sensor capable of deployment in a variety of positions. It generates a rich data set, of potential value for control and monitoring of machine operation as well as for diagnostic purposes. For example, the active tracking of the rotational frequency during the startup phase could be utilized by the rotor control system to improve machine control and prevent overshoot. There are many possibilities for further diagnostic analysis of the rotor system based on the amplitude time series generated for each of the signal components.

References

[1] C.J. Stander, P.S.Heyns, W.Schoombie, Using vibration monitoring for local fault detection on gears operating under fluctuating load conditions, Mech. Syst. Signal Process. 16(6) (2002) 1005–1024, DOI: 10.1006/mssp.2002.1479.

[2] F. Combet, L. Gelman, An automated methodology for performing time synchronous averaging of a gearbox signal without speed sensor, Mechanical Systems and Signal Processing, Volume 21, Issue 6, 2007, pp 2590-2606, DOI: 10.1016/j.ymssp.2006.12.006.

[3] Kiran Vernekar, Hemantha Kumar, K.V. Gangadharan, Gear Fault Detection Using Vibration Analysis and Continuous Wavelet Transform, Procedia Materials Science, Vol. 5, 2014, pp 1846-1852, DOI: 10.1016/j.mspro.2014.07.492.

[4] M. Feldman, Hilbert transform in vibration analysis, Mech. Syst. Signal Process., 25(3), 2011, pp 735-802, DOI: 10.1016/j.ymssp.2010.07.018

[5] Gang Cheng, Xihui Chen, Hongyu Li, Peng Li, Houguang Liu, Study on planetary gear fault diagnosis based on entropy feature fusion of ensemble empirical mode decomposition, Measurement, Vol. 91, 2016, pp 140-154, DOI: 10.1016/j.measurement.2016.05.059.

[6] M.A. Jafarizadeh, R. Hassannejad, M.M. Ettefagh, S. Chitsaz, Asynchronous input gear damage diagnosis using time averaging and wavelet filtering, Mech. Syst. Signal Process., Vol. 22, 2008, pp 172-201, DOI: 10.1016/j.ymssp.2007.06.006.

[7] M. Amarnath, I.R. Praveen Krishna, Local fault detection in helical gears via vibration and acoustic signals using EMD based statistical parameter analysis, Measurement, Vol. 58, 2014, pp 154-164, DOI: 10.1016/j.measurement.2014.08.015

[8] Yu Yang, Yigang He, Junsheng Cheng, Dejie Yu, A gear fault diagnosis using Hilbert spectrum based on MODWPT and a comparison with EMD approach, Measurement, Vol. 42, 2009, pp 542-551, DOI: 10.1016/j.measurement.2008.09.011

[9] F.Bonnardot, M.El Badaoui, R.B.Randall, J.Danière, F. Guillet, “Use of the acceleration signal of a gearbox in order to perform angular resampling (with limited speed fluctuation)”, Mechanical Systems and Signal Processing, Vo. 19, Issue 4, July, 2005, pp.766-785.

[10] S. Lu, J. Guo, Q. He, “A Novel Contactless Angular Resampling Method for Motor Bearing Fault Diagnosis Under Variable Speed”, IEEE Transactions on Instrumentation and Measurement, Vol. 65, Issue 11, Nov. 2016, pp. 2538 – 2550, DOI: 10.1109/TIM.2016.2588541

[11] V. Sinitsin and A. L. Shestakov, “Wireless acceleration sensor of moving elements for condition monitoring of mechanisms”, Meas. Sci. Technol. 28 (2017) 094002. DOI: 10.1088/1361-6501/AA7AB6

[12] Sinitsin, V.V. “Roller bearing fault detection by applying wireless sensor of instantaneous accelerations of mechanisms moving elements”. 15th IMEKO TC10 Workshop on Technical Diagnostics 2017 - "Technical Diagnostics in Cyber-Physical Era", Budapest, June, 2017.

[13] M.P. Henry, F. Leach, M. Davy, O. Bushuev, M.S. Tombs, F. B. Zhou, and S. Karout, “The Prism: Efficient Signal Processing for the Internet of Things”, IEEE Industrial Electronics Magazine, pp 2–10, December 2017. DOI: 10.1109/MIE.2017.2760108.

[14] Henry, MP, Sinitsin, VV. “Prism Signal Processing for Machine Condition Monitoring I: Design and Simulation”, 1st IEEE International Conference on Industrial Cyber-Physical Systems (ICPS 2018) Saint Petersburg, Russia, 2018.

[15] Henry, MP. “An Introduction to Prism Signal Processing applied to Sensor Validation”, Measurement Techniques, pp 1233 – 1237, Mar 2018. DOI: 10.1007/s11018-018-1345-1